

## Large complete band gap in two-dimensional photonic crystals with elliptic air holes

Min Qiu and Sailing He

*Department of Electromagnetic Theory, Royal Institute of Technology, 100 44 Stockholm, Sweden*

(Received 8 April 1999)

It is shown that elliptic air holes can be used effectively as inclusions to obtain a large complete band gap for two-dimensional photonic crystals. An instructive procedure of how one quickly finds the optimal configuration which gives the maximum complete band gap is described. [S0163-1829(99)12839-X]

Intensive investigations have been carried out recently on photonic crystals in view of their potential usefulness in controlling light propagation (cf., e.g., Refs. 1–4). If, for some frequency range, a photonic crystal reflects light of any polarization totally at any incident angle, the crystal is said to have a complete photonic band gap (PBG). In such a photonic crystal, no light modes can propagate if the frequency is within that PBG range. By using line defects (i.e., carving a waveguide out of an otherwise perfect photonic crystal), one can guide light from one location to another. Once light is induced to travel along this waveguide, it has nowhere else to go as the mode is forbidden to escape into the crystal. Based upon the above ideas, a photonic crystal fiber has been fabricated by, e.g., making (through a stack and draw procedure) a hexagonal array (except at the center grid point) of air holes in a long silica matrix, with a dielectric core at the center.<sup>5,6</sup> The center core then serves as a line defect in a photonic crystal environment. In other words, a photonic crystal fiber uses a two-dimensional (2D) photonic crystal as the fiber cladding. If the parameters are chosen properly, such a photonic crystal fiber provides the possibility of controlling light in novel ways which are impossible in a conventional optical fiber. Motivated by the application of photonic crystal fibers, we consider in the present paper only 2D photonic crystals with air holes as inclusions.

To obtain a larger PBG for circular inclusions in a rectangular lattice, two sets of inclusions<sup>7</sup> and anisotropic inclusions<sup>8</sup> have been used. However, these are not convenient for fabrication of photonic crystal fiber. In the present paper, we wish to reach a similarly large PBG by using elliptic (instead of circular) air holes in a rectangular lattice. A rectangular array of elliptic air holes (identically same) can be made easily in an isotropic background dielectric medium (gallium arsenide or silica) in the fabrication of photonic crystal cladding for a photonic crystal fiber.

Consider an infinite periodic rectangular grid with period  $l_x$  along the  $x$  direction and period  $l_y$  along the  $y$  direction, see Fig. 1. We choose the  $y$  direction to be the one with larger period (i.e.,  $l_y \geq l_x$ ). Denoted by  $s$  as the ratio of the two periods, i.e.,  $s = l_x/l_y$ , then  $s$  has a value between 0 and 1.0. Denote the half-axes of the elliptic air holes by  $a$  (long half-axis) and  $b$  (minor half-axis). The dielectric constant for the background material is denoted by  $\epsilon_b$ .

The band structure for such a photonic crystal can be calculated by the standard plane-wave expansion method.<sup>9–13</sup> In the present paper, we use 441 plane waves, and the computational error was estimated to be less than 1% for the lowest 10 photonic bands.

In order to compare our PBG results with the ones given in Refs. 7 and 8, we start our study by using the same background material—gallium arsenide, which has a dielectric constant of  $\epsilon_b = 11.4$ .<sup>2,14</sup> A 2D photonic crystal with a triangular lattice of air holes on gallium arsenide has been fabricated.<sup>15</sup>

Figure 2 shows the calculated photonic band structure for circular air holes in a rectangle lattice with  $s = 0.77$  and radius  $r = 0.38l_y$  [this configuration actually is obtained in step 1 of the procedure (described below) of finding the optimal configuration which gives the maximum complete band gap]. The filling fraction for the air holes is  $f = 0.59$ . In the present case the irreducible Brillouin zone is a rectangular box, rather than the triangular wedge for the case of square lattice with circular air holes. The rest of the Brillouin zone can be related to this rectangle box by rotational symmetry. Therefore, we have four special points,  $\Gamma$ ,  $X$ ,  $M$ , and  $X'$  corre-

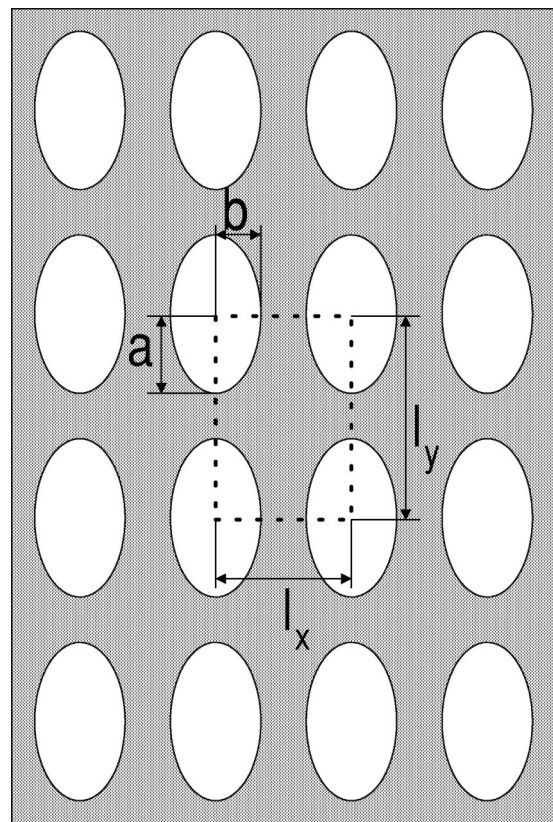


FIG. 1. A 2D periodic rectangular array of elliptic air holes in a background material.

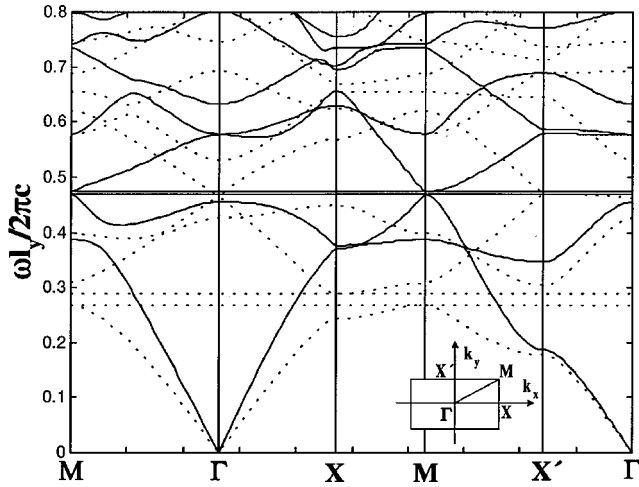


FIG. 2. Band structure for a 2D photonic crystal with circular air holes on gallium arsenide material ( $\epsilon_b = 11.4$ ). The period ratio is  $l_x/l_y = 0.77$ , and the radius is  $r (= a = b) = 0.38l_y$ . The solid curves are for the  $H$  polarization, and the dotted curves are for the  $E$  polarization.

sponding respectively to  $\mathbf{k}_{\parallel} = 0$ ,  $\mathbf{k}_{\parallel} = \pi/l_x \hat{x}$ ,  $\mathbf{k}_{\parallel} = \pi/l_x \hat{x} + \pi/l_y \hat{y}$  and  $\mathbf{k}_{\parallel} = \pi/l_y \hat{y}$ . In Fig. 2, the solid curves are for the  $H$  polarization, and the dotted curves are for the  $E$  polarization. From this figure one sees that a complete band gap does not exist in this case (this has been shown earlier by others; see, e.g., Ref. 2). The band gap of  $H$ -polarization modes is between the second and the third band, and the center frequency is around  $0.47(2\pi c/l_y)$ . The center frequency for the 1-2 band gap of  $E$  polarization modes is around  $0.28(2\pi c/l_y)$ , which is much lower than the center frequency for the  $H$  2-3 mode. The two band gaps have no overlap. If we can move the  $H$  2-3 band gap downwards, or move the  $E$  1-2 band gap upwards, a complete band gap can be obtained. A large complete PBG usually requires a large filling fraction for the inclusions. In order to obtain a larger filling fraction for the air holes, we put the long axis of the elliptic air holes along the  $y$  direction (along which it has a longer period in the 2D periodic structure) and increase the long half-axis  $a$ . From Ref. 2 we know that the first band (at low frequencies) of the  $E$  polarization has most of its energy in the dielectric regions, while the second band (with higher frequencies) has most of its energy in the air regions. Thus, as the long axis  $a$  increases (i.e., the area of the air regions increases), the energy in the air regions increases, and the second band moves towards higher frequencies. Consequently, the  $E$  1-2 band gap moves upwards. The same physical explanation holds for the  $H$  polarization. Our numerical results also indicate that both the  $E$  1-2 band gap and the  $H$  2-3 band gap move upwards as the long half-axis  $a$  increases, and furthermore, the  $H$  2-3 band gap moves a bit faster than the  $E$  1-2 band gap. Therefore, we cannot find a complete (i.e., overlapped) band gap between these two band gaps (the  $E$  1-2 band gap increases as  $a$  increases, however, it never reaches a level that makes an overlap with  $H$  2-3 band gap possible). The rule of thumb for photonic band gaps<sup>2</sup> indicates that  *$E$ -polarization band gaps are favored in a lattice of isolated high- $\epsilon$  regions, and  $H$ -polarization band gaps are favored in a connected lattice*. Thus, one may find other band gaps for the  $E$ -polarization, besides the  $E$  1-2

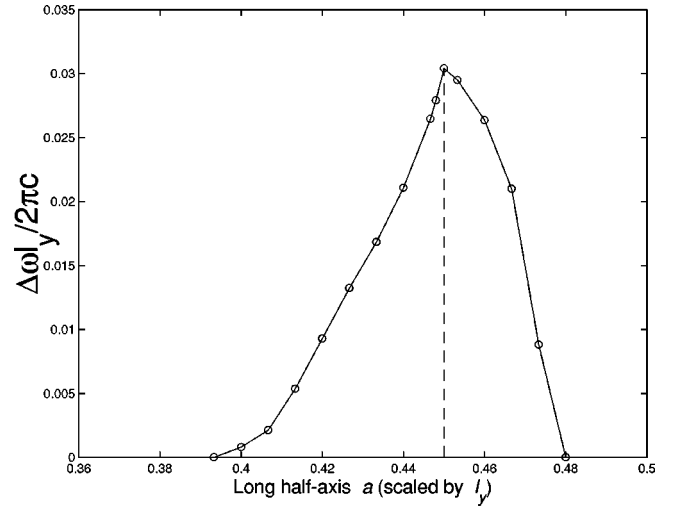


FIG. 3. The width of the complete band gap as the long half-axis  $a$  varies. The period ratio is  $l_x/l_y = 0.77$ , and the minor half-axis is  $b = 0.38l_y$ .

band gap. Our numerical results indicate that there exists an  $E$ -polarization band gap between the third and fourth bands as the long axis  $a$  increases. If we can let the  $H$  2-3 band gap overlap with the  $E$  3-4 band gap, we can achieve a complete band gap. From Fig. 2 one sees that the  $E$  3-4 band gap is very small compared with the  $H$  2-3 band gap in the case of circular air holes. Therefore, we increase the long half-axis  $a$  of the elliptic air holes to obtain a larger  $E$  3-4 band gap.

Following this idea, and also considering the fact that both  $H$  2-3 and  $E$  3-4 band gaps move upward as the long half-axis  $a$  of the elliptic air holes increases, we proceed with the following two steps in order to find a suitable period ratio  $s$ , and half-axes  $a$  and  $b$  of the elliptic air holes which give an optimal complete band gap [we use gallium arsenide ( $\epsilon_b = 11.4$ ) as an example to illustrate the procedure below].

Step 1. Find a suitable period ratio  $s$  and radius  $r$  of circular air holes (i.e.,  $a = b = r$ ) for which the center frequency of the  $H$  2-3 band gap and that of the  $E$  3-4 band gap are at a similar level. This is because both the  $H$  2-3 and  $E$  3-4 band gaps move upwards with a similar speed as  $a$  increases (this can be checked easily by a numerical perturbation method). Our numerical simulation gives  $s = 0.77$  and  $r = 0.38l_y$ . The corresponding band structure is shown in Fig. 2. From this figure one sees that the center frequency of the  $H$  2-3 band gap and that of the  $E$  3-4 band gap are at a similar level (though both band gaps are quite narrow).

Step 2. Fix the period ratio  $s$  and  $b = r$ , but increase the long half-axis  $a$  to an optimal value. The width of the complete band gap as  $a$  increases is shown in Fig. 3. When  $a$  is greater than  $0.40l_y$ , the complete band gap appears. The complete band gap reaches its maximum value  $\Delta\omega = 0.0304(2\pi c/l_y)$  when  $a$  is at about  $0.45l_y$ . The corresponding band structure is shown in Fig. 4, where the complete band gap is indicated by the shaded area.

This complete band gap has reached a level similar to the one reported in Refs. 7 and 8 where complicated configurations (two sets of inclusions or anisotropic circular inclusions) were used. If  $a$  increases further, the complete band gap decreases quite sharply. This is due to the following two reasons. Firstly, the  $H$ -polarization band gap disappears as  $a$

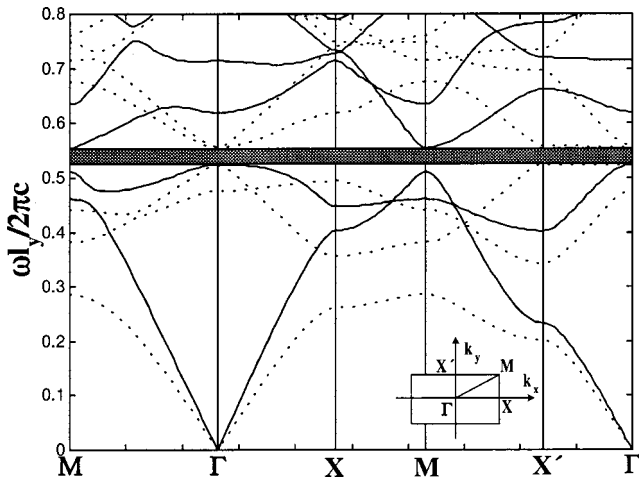


FIG. 4. The band structure with the optimal complete photonic band gap for elliptic air holes in gallium arsenide material. The optimal configuration has the following parameters:  $l_x/l_y=0.77$ ,  $a=0.45l_y$ ,  $b=0.38l_y$ . The solid curves are for the  $H$  polarization, and the dotted curves are for the  $E$  polarization. The complete band gap is indicated by the shaded area.

increases. As we know,  $H$ -polarization band gaps are favored in a connected high- $\epsilon$  material lattice. When  $a$  is close to  $0.50l_y$ , the connected high- $\epsilon$  region becomes small, and thus the  $H$ -polarization band gap disappears. Secondly, the up-moving speed of the  $H$ -polarization band is a bit faster than that of the  $E$ -polarization band, and thus the position of the  $H$  2-3 band gap exceeds that of the  $E$  3-4 band gap for larger  $a$ .

The final photonic band structure with an optimal PBG for elliptic air holes in gallium arsenide is shown in Fig. 4. From this figure one sees clearly that the  $H$  2-3 band gap overlaps almost fully with the  $E$  3-4 band gap [the  $H$  2-3 band gap is between  $0.5241$  and  $0.5548$  ( $2\pi c/l_y$ ), and  $E$  3-4 band gap is between  $0.5224$  and  $0.5545$  ( $2\pi c/l_y$ )]. If we choose the wavelength  $\lambda=2\pi c/\omega=1.5\ \mu\text{m}$  in an application, then it requires  $\omega l_y/2\pi c=l_y/\lambda=l_y/1.5\ \mu\text{m}\approx 0.53$ , i.e.,  $l_y\approx 0.8\ \mu\text{m}$  (and thus  $l_x\approx 0.616\ \mu\text{m}$ ,  $a=0.36\ \mu\text{m}$ , and  $b=0.304\ \mu\text{m}$ ). The PBG corresponds to a stop band from wavelength  $\lambda=1.44\ \mu\text{m}$  to  $\lambda=1.53\ \mu\text{m}$ .

Following the same procedure, we have also investigated

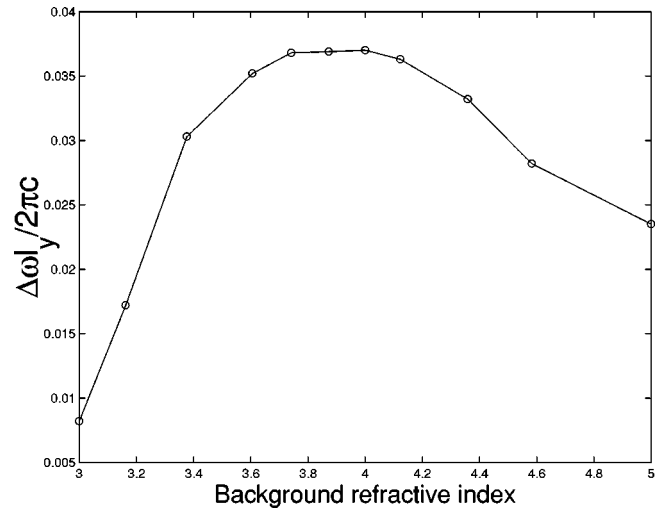


FIG. 5. Optimal complete photonic band gap for 2D photonic crystals with inclusions of elliptic air holes as the refractive index of the background material varies.

the optimal complete band gap for elliptic air holes in other dielectric background materials. In Fig. 5 we plot the optimal complete band gap as a function of the refractive index (in the range of  $3.0\leq n\leq 7.0$ ). The optimal complete band gap increases as the refractive index increases, and reaches its maximum value  $\Delta\omega=0.0370(2\pi c/l_y)$  when the refractive index is around 4 (i.e.,  $\epsilon_b\approx 16$ ; the dielectric constant of semiconductor Germanium is around 16).<sup>14</sup> The complete band gap then decreases as the refractive index increases further. The dielectric constant for semiconductor silicon is around 11.7,<sup>14</sup> and thus the PBG behaviors for elliptic air holes in silicon are quite similar to the ones shown in Figs. 2–4.

In conclusion, we have shown that inclusions of elliptic air holes can be used effectively to obtain a larger complete band gap for 2D photonic crystals. We have described how to quickly find the optimal configuration which gives the maximum complete band gap. Such a 2D photonic crystal is very convenient for use as cladding for a photonic crystal fiber.

The partial support of the Wenner-Gren Foundation for this project is gratefully acknowledged.

<sup>1</sup>E. Yablonovitch, Phys. Rev. Lett. **58**, 2059 (1987).

<sup>2</sup>J. D. Joannopoulos, R. D. Mead, and J. N. Winn, *Photonic Crystals: Molding the Flow of Light* (Princeton University Press, Princeton, 1995).

<sup>3</sup>*Photonic Band Gaps and Localization*, Proceedings of the NATO ARW, edited by C. M. Soukoulis (Plenum Press, New York, 1993).

<sup>4</sup>J. D. Joannopoulos, P. R. Villeneuve, and S. Fan, Nature (London) **386**, 143 (1997).

<sup>5</sup>J. C. Knight, T. A. Birks, P. St. J. Russell, and D. M. Atkin, Opt. Lett. **21**, 1547 (1996).

<sup>6</sup>J. C. Knight, T. A. Birks, P. St. J. Russell, and J. P. de Sandro, J. Opt. Soc. Am. A **15**, 748 (1998).

<sup>7</sup>C. M. Anderson and K. P. Giapis, Phys. Rev. Lett. **77**, 2949

(1996).

<sup>8</sup>Z. Y. Li, B. Y. Gu, and G. Z. Yang, Phys. Rev. Lett. **81**, 2574 (1998).

<sup>9</sup>K. M. Ho, C. T. Chan, and C. M. Soukoulis, Phys. Rev. Lett. **65**, 3152 (1990).

<sup>10</sup>K. M. Leung and Y. F. Liu, Phys. Rev. Lett. **65**, 2646 (1990).

<sup>11</sup>Z. Zhang and S. Satpathy, Phys. Rev. Lett. **65**, 2650 (1990).

<sup>12</sup>M. Plihal and A. A. Maradudin, Phys. Rev. B **44**, 8565 (1991).

<sup>13</sup>M. Plihal, A. Shambrook, and A. A. Maradudin, Opt. Commun. **80**, 199 (1991).

<sup>14</sup>J. I. Pankove, *Optical Processes in Semiconductors* (Dover, New York, 1971).

<sup>15</sup>J. R. Wendt, G. A. Vawter, P. L. Gourley, T. M. Brennan, and B. E. Hammons, J. Vac. Sci. Technol. B **11**, 2637 (1993).